

# DESIGN OF BEAM TRANSPORT LINES FOR RADIOISOTOPE PRODUCTION SYSTEMS IN NIRS CYCLOTRON FACILITY

Ken Katagiri\*, Satoru Hojo, Masao Nakao, Akinori Sugiura, Kazutoshi Suzuki, Akira Noda, Koji Noda, NIRS, Chiba, Japan

## Abstract

A new beam transport and a irradiation system were designed for radionuclides production with heat damageable targets. The incident beam is swept along a circle on the irradiation target with fast steering magnets. The width and the sweeping radius of the incident beams were optimized to achieve high production efficiency and avoid the heat damages. Based on those optimized parameters, beam optics of the new beam transport lines was optimized. To obtain initial conditions for the optical calculations, the beam emittance and the Twiss parameters were measured at the upper stream of the new beam transport lines. In this paper, we present the results of the calculations and the optimized beam transport lines.

## INTRODUCTION

The cyclotron facility at the NIRS (National Institute of Radiological Sciences) is composed of a NIRS 930 cyclotron (AVF 930, Thomson-CSF) and a small cyclotron (HM-18, Sumitomo Heavy Industries, Ltd.) [1, 2]. The NIRS 930 cyclotron has been dedicated to produce radionuclides for researches in nuclear medicine, and perform fundamental physics/biology experiments. The radionuclide production is also performed with the small cyclotron to diagnose patients treated by heavy-ion cancer therapy using Heavy-Ion Medical Accelerator (HIMAC) synchrotron.

The NIRS 930 cyclotron provides ion beams to totally seven beam transport lines. Three of them are used for the fundamental physics/biology experiments, and other two beam transport lines are used for production of the radionuclides. In recent years, production of radionuclides emitting alpha particles, such as an At-211, are expected to be started with a new target system for new researches related to the unsealed radionuclide therapy. Also, we are planning to perform production experiments of  $^{10/11}\text{CH}_4$  molecules, related to the heavy-ion cancer therapy [3]. To perform those new experiments, new beam transport lines are required.

In the production experiments of  $^{10/11}\text{CH}_4$  molecules, sodium borohydride ( $\text{NaBH}_4$ ) was proposed to be used for a proton irradiation target. In previous work, we found that  $^{10/11}\text{C}$  nuclides could be effectively collected with proton beams ( $^{10/11}\text{B}$  (p,n)  $^{10/11}\text{C}$ ) owing to solid-state hydrogen atoms. However, the target was easily damaged by heating with the proton irradiation. The damage of the target leads to degradation of the production efficiency. For those heat damageable targets, we investigated a method to form ir-

radiation field using fast combined steering magnets. The irradiation beams are swept by the steering magnets along a circle on the irradiation target to broaden the beam profile. We investigated the beam width and the radius of the swept area circle where the proton beam is swept on the target to obtain high production efficiency and avoid the heat damages. Then, we considered the layout of the new beam transport line and optimized its optical functions to achieve the desired beam width and the radius of the circle. To obtain initial conditions for the optical calculations, the beam emittance and the Twiss parameters were experimentally measured at the upper stream of the new beam transport lines. In this paper, we present the results of the calculations and the optimized beam transport lines.

## IRRADIATION FIELD FORMATION

Figure 1 shows the layout of the beam transport line considered in this study. The transport line in the first floor already exists and has been also used for the radionuclide production. In this study, we design the transport line starting from the entrance of the beam transport (B.T.) to the "port A" in the basement floor, as shown in Fig. 1.

Figure 2 shows a schematic diagram of a target box and the irradiation beam broadened with the combined steering magnets shown in Fig. 1. The target materials are enclosed in the target box and irradiated by the broad beam. The time period required to melt 1-g  $\text{NaBH}_4$  target using 30-MeV,  $20\text{-}\mu\text{A}$  proton beam is estimated to be  $\sim 1$  (s) from its specific heat of about 90 (J/mol/K). The swept beam can thus be considered as a constant-broad beam when the frequency of the sweeping magnets are much higher than 1 Hz. Although the wobbling method [4] used for particle cancer therapy often employs a scatterer, we considered a

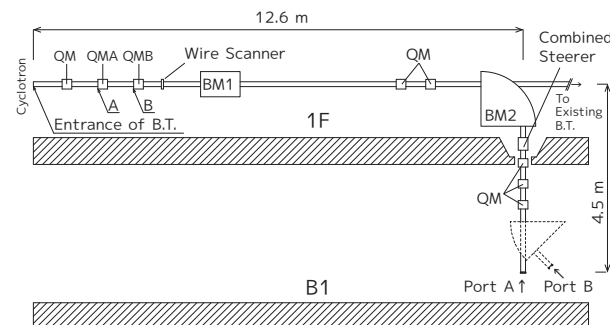


Figure 1: Layout of the beam transport line from the NIRS 930 cyclotron. BM1 and BM2 are the horizontal 2.5-degree dipole magnet and the vertical 90-degree dipole magnet, respectively.

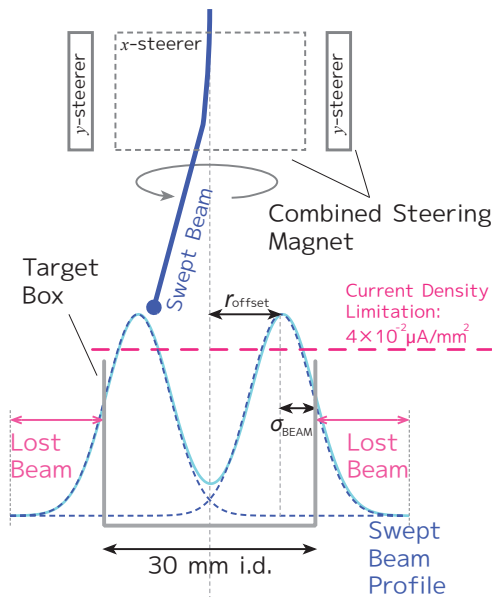


Figure 2: Irradiation field formation using fast combined steering magnets.

irradiation system without the scatterer to avoid energy loss and omit its cooling system.

The beam width  $\sigma_{\text{beam}}$  and the offset radius  $r_{\text{offset}}$  were determined to satisfy the following two conditions: (1) current density of the incident beam  $i_{\text{beam}}$  is less than  $4 \times 10^{-2} \mu\text{A}/\text{mm}^2$ , (2) irradiation efficiency  $\varepsilon_{\text{beam}}$  is as high as possible to increase the yield of the radionuclide and avoid undesirable activation of the target box. The upper limit of the current density was determined to be the highest current that does not melt the  $\text{NaBH}_4$  target [3]. The irradiation efficiency  $\varepsilon_{\text{beam}}$  is defined as a ratio of beam current irradiating the target to the total beam current. The irradiation efficiency  $\varepsilon_{\text{beam}}$  is degraded by the lost beam shown in Fig. 2. In this investigation, we considered a target box with inner diameter of 30 mm.

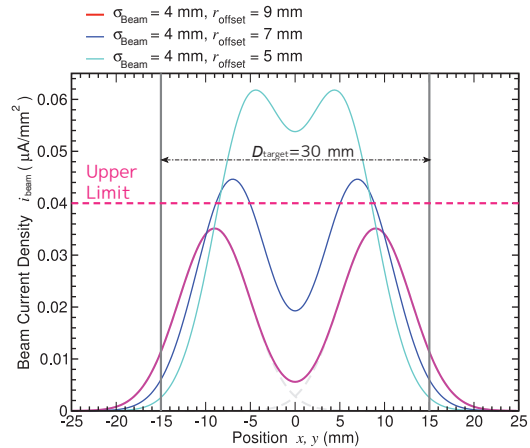


Figure 4: Beam profile for  $(\sigma_{\text{beam}}, r_{\text{offset}}) = (4 \text{ mm}, 9 \text{ mm})$ . Beam profiles for  $r_{\text{offset}} = 5$  and 7 mm are also plotted as a reference.

ation efficiency  $\varepsilon_{\text{beam}}$  is degraded by the lost beam shown in Fig. 2. In this investigation, we considered a target box with inner diameter of 30 mm.

To determine the  $\sigma_{\text{beam}}$  and  $r_{\text{offset}}$ , the irradiation efficiency  $\varepsilon_{\text{beam}}$  and current density of the incident beam  $i_{\text{beam}}$  were calculated for the wide range of  $0 \leq \sigma_{\text{beam}}, r_{\text{offset}} \leq 15 \text{ mm}$ , as shown in Fig. 3. It was difficult to obtain high irradiation efficiency higher than 90% when using the 30-mm diameter target box. To satisfy the two conditions of (1) and (2), we choose a point of  $(\sigma_{\text{beam}}, r_{\text{offset}}) = (4 \text{ mm}, 9 \text{ mm})$ , as indicated by a star in Fig. 3. A beam profile for the obtained condition is plotted in Fig. 4. Beam profiles for  $r_{\text{offset}} = 5$  and 7 mm are also plotted as a reference. Although the uniformity of those profiles are rather rough compared to that used for the cancer treatment [4], the beam profile can be expected to be suitable for radionuclides production with the heat damageable targets.

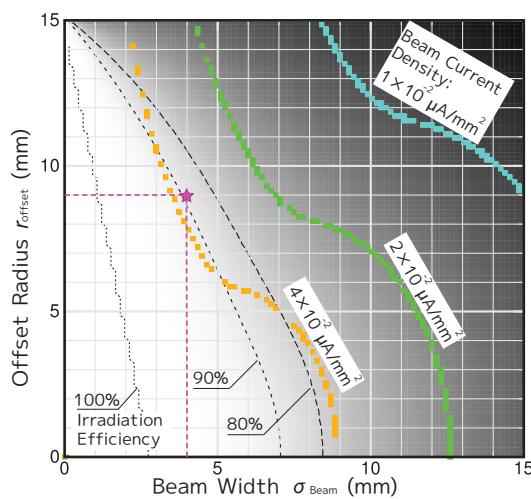


Figure 3: Contour map showing the irradiation efficiency  $\varepsilon_{\text{beam}}$  (black/white) and the current density of the incident beam  $i_{\text{beam}}$  (turquoise/green/orange).

## TWISS PARAMETER MEASUREMENTS AND BEAM OPTICS

To perform the optical calculation and the optimization, Twiss parameters at the entrance of the beam transport (Fig. 1) have to be determined. Also the emittance is required for the calculation of the envelopes. Thus, we measured those parameters by the Q-scan method. The horizontal Twiss parameters at the point "B" in Fig. 1 and horizontal emittance were measured by changing the strength of the quadrupole magnet "QMB". Also, the vertical Twiss parameters at the point "A" and vertical emittance were measured with the change of the quadrupole magnet "QMA". The beam size measurements were performed with a wire scanner installed at the downstream of those two magnets. Figure 5 shows the fitting result of the Q-scan measurement for horizontal Twiss parameters. Because the variable  $c$  of the fitted quadratic function could not be analyzed well ( $\sigma_{\text{error}}/c \sim 100\%$ ), it was derived

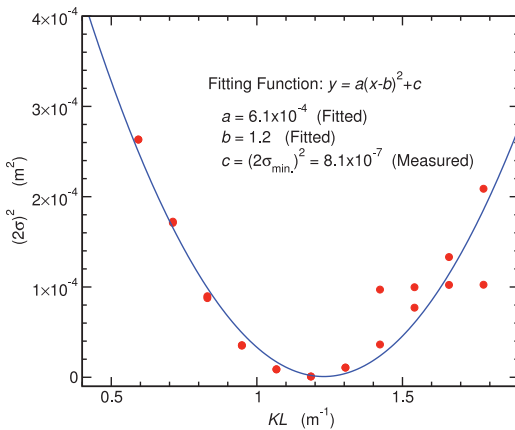


Figure 5: Fitting result of Q-scan measurement for horizontal Twiss parameters.

from the minimum value of the beam width measured by the wire scanner. From those measured values, Twiss parameters at the entrance of the beam transport were derived by using transfer matrices, as shown in Table 1. Those twiss parameters were used for as initial conditions of the optical calculation. Also, by using a well known equation [5], the initial condition of horizontal dispersion  $D_x$  was roughly estimated to be  $D_x \simeq -R_{\text{ext}}/\gamma^2 = -0.9$  (m) for the 30-MeV proton. Here the  $R_{\text{ext}}$  is the extraction radius of the NIRS 930 cyclotron. The other parameters were assumed to be  $D_y, D'_x, D'_y = 0$ . To optimize the field gradient strength of the quadrupole magnets, following constraint conditions at the target box were employed for the optical matching:  $\sqrt{\beta_x \varepsilon_x}, \sqrt{\beta_y \varepsilon_y} = 4$  mm (evaluated condition shown in Fig. 3),  $D_x, D_y = 0$ .

Figure 6 shows horizontal and vertical dispersion functions obtained by the optical matching. The constraint condition for the dispersion function at the target could be successfully satisfied. With those dispersion functions, the calculated momentum spread of  $\Delta p/p \simeq 1.5 \times 10^{-3}$  [6], the beta functions obtained by the optical matching, and the emittance shown in Table 1, the envelope functions were

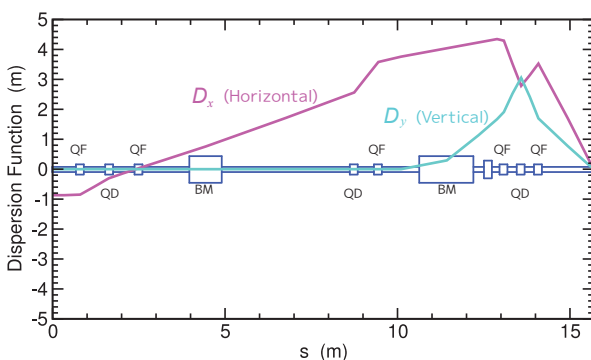


Figure 6: Horizontal and vertical dispersion functions for the new beam transport.

Table 1: Results of Twiss parameter and emittance measurements. Measurements were performed for 30-MeV proton beams.

	Twiss parameters at the entrance of B.T.	2σ emittance of 30-MeV proton $\varepsilon$ ( $\pi$ mm mrad)
	$\alpha$	$\beta$ (m)
Horizontal	-8.2	11.9
Vertical	-2.7	8.7

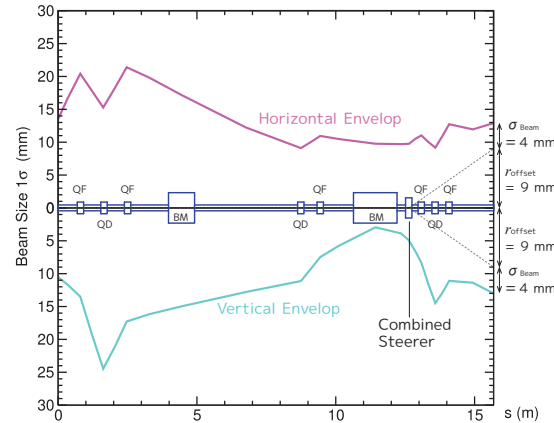


Figure 7: Horizontal and vertical envelope functions with kicks produced by the fast combined steering magnets. The kicked beam axis is shown with a broken line. The kick angle is  $\theta \simeq 3$  mrad.

evaluated as shown in Fig. 7. We confirmed that the beam profile at the target box achieved the desired condition for radionuclides production using the heat damageable targets and the 30-mm diameter target box.

## CONCLUSION

A new beam transport for the NIRS 930 cyclotron was investigated for the heat damageable irradiation target used for the radionuclides production. To more properly determine the beam optics, we are planning to measure the dispersion function at the entrance of the beam transport.

## REFERENCES

- [1] T. Honma, et al., Proc. 18th Int. Conf. on Cyclotrons and their Applications 2007, Oct. 1-15, 2007, Giardini Naxos, Italy, p137-139.
- [2] S. Hojo, et al., in these proceedings.
- [3] K. Katagiri, K. Nagatsu, et al., Rev. Sci. Instrum. 85 (2014) 02C305-1.
- [4] W.T. Chu, S.B. Curtis, et al., IEEE Trans. Nucl. Sci 32 (1985) 3321.
- [5] M. Seidel, CERN Yellow Reports 2013-001 (2000) 17.
- [6] M. Nakao, et al., in these proceedings.